

The following article is the final version submitted to IEEE after peer review; hosted by PTB;
DOI: [10.7795/EMPIR.17IND06.CA.20191122](https://doi.org/10.7795/EMPIR.17IND06.CA.20191122). It is provided for personal use only.

Setup and Characterisation of Reference Current-to-Voltage Transformers for Wideband Current Transformers Calibration up to 2 kA

Y. Chen, E. Mohns, H. Badura, P. R  ther and M. Luiso

Acknowledgement: The presented work is used in the project 17IND06 (FutureGrid II) which have received funding from the EMPIR programme co-financed by the Participating States and from the European Union's Horizon 2020 research and innovation programme.

  2018 IEEE. This is the author's version of an article that has been published by IEEE. Personal use of this material is permitted. Permission from IEEE must be obtained for all other uses, in any current or future media, including reprinting/republishing this material for advertising or promotional purposes, creating new collective works, for resale or redistribution to servers or lists, or reuse of any copyrighted component of this work in other works.

Full Citation of the original article published by IEEE:

Y. Chen, E. Mohns, H. Badura, P. R  ther and M. Luiso, "Setup and Characterisation of Reference Current-to-Voltage Transformers for Wideband Current Transformers Calibration up to 2 kA," *2019 IEEE 10th International Workshop on Applied Measurements for Power Systems (AMPS)*, Aachen, Germany, 2019, pp. 1-6.
DOI: 10.1109/AMPS.2019.8897759

Available at:

<http://ieeexplore.ieee.org/stamp/stamp.jsp?tp=&arnumber=8897759&isnumber=8897706>

Setup and Characterisation of Reference Current-to-Voltage Transformers for Wideband Current Transformers Calibration up to 2 kA

Y. Chen[#], E. Mohns[#], H. Badura[#], P. Räther[#] and M. Luiso^{*}

[#]Physikalisch-Technische Bundesanstalt (PTB), Bundesallee 100, Braunschweig, Germany

^{*}Dept. of Engineering, University of Campania “Luigi Vanvitelli”, Aversa (CE), Italy

Abstract— This paper describes the setup and characterisation of a set of wideband Current-to-Voltage (C-to-V) transformers equipped with a symmetrical winding arrangement on its primary side. The transformer set is being developed at PTB and contributes to the European project “FutureGrid II – metrology for the next-generation digital substation instrumentation”. The objective of this paper was to use the reference transformer to calibrate the digital instrument transformer (IT) not only accurately at power frequency but also stably within a wider bandwidth. The calibrated errors of the first current transformer (CT), which is known as CT50, were within ± 5 ppm and μrad at 50 Hz. The uncertainty of the CT50 was $\pm 6 \cdot 10^{-6}$ for the ratio and phase errors ($k = 2$). The frequency response errors of the CT50 up to 12 kHz were below 0.1 % and 0.2 crad with the expanded uncertainties below $\pm 1 \cdot 10^{-4}$ for the ratio errors and $\pm 3 \cdot 10^{-4}$ for the phase errors ($k = 2$).

Keywords— wideband, current transformers, calibration, measurement uncertainty, instrument transformers, power quality

I. INTRODUCTION

The first generation of analogue measurement and control systems in traditional power grid substations is approaching the end of their favourable lifespan. According to IEC 61850, digital measurements are gradually coming into use in substations.[1] The European project “Future grid II” is aimed at providing hitherto missing solutions for the calibration and timing of the new type of substation instrumentation. In general, electricity transmission and distribution systems concern about Power Quality (PQ) [2] and Phasor Measurement Units (PMUs) monitoring from general metering to protection and grid diagnostics. Precise measurements of grid voltage and current are required for all static, dynamic and transient PQ / PMU test events. Some recent literatures [3], [4] show that inductive ITs suffer from an intrinsic nonlinearity which is responsible for uncertainties up to some percent when measuring PQ phenomena.

In the case of changing traditional analogue IT technology to the new digital instrumentation technology on transmission and distribution level, new reference systems which are able to calibrate digital IT even under dynamic and transient test voltages and currents. To enable this, the reference transformers must be sufficiently linear and should work ideally in bandwidth from DC up to the highest frequencies of the tested dynamic signals. Hence, a realisation of the new reference

system is supposed to characterise digital IT not only at stationary signals at 50 Hz but also within a wider bandwidth, so the system is compatible with further technical specifications of the standards [5], [6]. Based on the new reference standards and systems, calibrated digital IT can be used in digitally equipped substations for accurate PQ / PMU measurements with intelligent electronic devices, such as digital energy meters or real-time critical all-digital PMUs.

One of the objectives of FutureGrid II is to develop new reference standards and calibration systems for the dynamic calibration of digital instrument transformers with currents of at least 2 kA. In order to achieve this, a new calibration system is required which contains a suitable high current generation with an analogue amplifier and a generation transformer-based source, a set of analogue reference C-to-V transformers and a precision measuring system. The measuring system is supposed to calibrate digital ITs and to evaluate its standard uncertainty according to the drafted IEC/IEEE TS 61869-105 [7] that the IEC TC38 / JWG55 started to work on in 2017. The precision measuring system has been investigated in a master thesis [8].

To convert an input current precisely into an output voltage, a CT with a precise measuring resistor on the secondary side, known as a C-to-V transformer, is preferred as a reference. Compared to a traditional highly stable calibration shunt [9], the C-to-V transformer allows the measuring resistor on its secondary side to operate with significantly less power. In this way, the current-to-voltage conversion can be easily carried out with high stability [10]. Another advantage is the fact that the CT has a galvanic isolation between its primary and secondary side.

In this paper, a set of four commercial zero-flux current transformers [11], [12] with rated currents from 50 A to 1500 A was used to establish the reference transformer set. To convert the secondary currents of this transformer set into an output voltage, a resistor box, containing precision resistors [13] from 1Ω to 20Ω was built. On the primary side of the zero-flux current transformers, a new symmetrical winding arrangement was designed and realised, which allows multiple current ranges. The characterisation of these reference transformers from 16 Hz to 12 kHz is presented in this paper.

II. SETUP OF THE C-TO-V TRANSFORMERS

The reference C-to-V transformer is made up of a commercial window type zero-flux transformer [11], [12] and a precision measuring resistor. To cover the current range up to 2 kA, a set of four CTs with rated currents of 50 A (CT50), 200 A (CT200), 600 A (CT600) and 2 kA (CT1500) was used. The rated current of the latter CT was relabelled after fixing the primary winding arrangement. To allow a better usage of the CTs, several current ranges were realised by adding several primary windings so that the number of turns could be selected. The measuring resistors were selected so that an output voltage of 1 V occurred at rated secondary current of the CTs. The realised rated primary currents of the C-to-V transformer set range from 8.3 A to 1500 A. The specific parameters of the C-to-V transformer set are listed in Table I with the different numbers of primary turns N_p , the rated primary and secondary currents, $I_{p,r}$ and $I_{s,r}$, and the nominal value of the measuring resistor R_m .

Table I: Parameters of the C-to-V transformer set

Type	N_p	$I_{p,r}$ in A	$I_{s,r}$	R_m (Ω)
CT50	1, ..., 6	8.3, ..., 50	100 mA	10 Ω
CT200	1, ..., 4	50, ..., 200	400 mA	2.5 Ω
CT600	1, ..., 4	150, ..., 600	400 mA	2.5 Ω
CT1500	1, ..., 3	500, ..., 1500	1 A	1 Ω

The maximum number of turns at the primary is determined so that each CT can be calibrated by its adjacent CT with the same primary input current. For instance, the CT50 with $N_p = 1$ is supposed to be the reference to calibrate the CT200 with $N_p = 4$. The rated primary current is 50 A. The secondary current $I_{s,r}$ of the CT remains the same in each current range. The measuring resistor is determined by $R_m = 1V / I_{s,r}$. The ratio F_{-iu} of the realised C-to-V transformer can be defined according to

$$F_{-iu} = \frac{U_S}{I_p} = \frac{R_m}{K_n} (1 + \varepsilon_m + \varepsilon_i) \cdot e^{j(\delta_m + \delta_i)} \quad (1)$$

where K_n is the rated current transformer ratio $I_{p,r} / I_{s,r}$, ε_i and δ_i represent the ratio errors and the phase errors of the CT, ε_m and δ_m represent the error of the of the measuring resistor and its phase error.

A. Winding arrangement of the Current Transformer

The usability and expected metrological characteristics of the window type zero-flux transformer were improved by implementation of several symmetrical primary windings of the CT. On the one hand, several primary windings allow the realisation of several current ranges for one CT, i.e., variable transformation ratios K_n . On the other hand, a two-dimensional symmetrical configuration of the primary windings enables a geometrically fixed measurement environment for the sake of obtaining stable and repeatable CT errors. In this way, the CT errors caused by the magnetic field of the primary windings are supposed to be constant as far as possible. Consequently, the CT errors are practically equal in each current range of the CT.

The symmetrical winding arrangement on the primary of the CT 50 is illustrated in detail in Fig. 1 (left). The other CTs (CT200, CT600, CT1500) follow a similar geometrical

arrangement with the corresponding practical parameters shown in Table I. From a vertical view, the whole CT (here the CT 50) consists of the window type CT itself, several wires for the primary windings, a winding support, which fixes the geometrical position of the primary wires and a connection box. The winding support and the connection box were fabricated with a 3D-printer. The connection scheme for the different primary windings $N_p = 1$ to 6 of the CT50 is shown in Fig. 1 (right). The port arrangement was designed to be symmetrically corresponding to the winding arrangement.

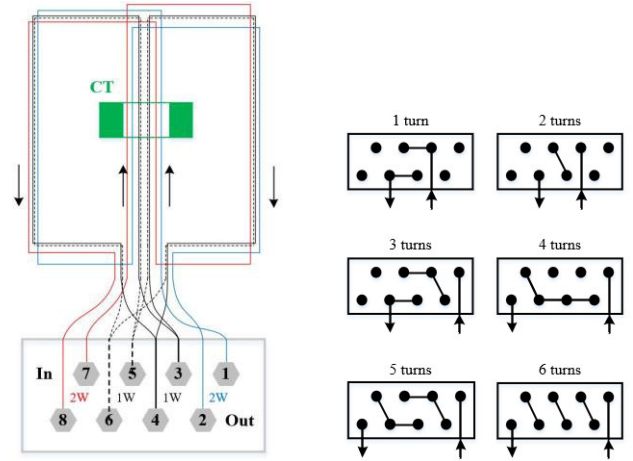


Fig. 1: Scheme of the primary winding arrangement (left) and port connection setups (right) of CT50.

The number of wires per turn, the number of turns for each port as well as the wire arrangement were considered and operated symmetrically. The arrow shows the direction of primary current flow of CT50. The ports in the upper row are input ports (Hi) and in the bottom row are the corresponding output ports (Lo). The left and right port pairs comprise two turns. The two centred port pairs comprise one turn. Here, each turn is realised with two wires, separately placed into the left and right side of the CT for getting symmetry. The input of the primary current for CT50 flows centrally through the hole of the CT, while its return current on the right and left side of the CT is divided into two identical parts.

Additionally, symmetry was applied to the wire coil in terms of its length, width and height. Length and height refer to the length and height of the centred wires and their two-side return wires. Width refers to the distance between the centred wires and their return. Theoretically, the magnetic field B of a wire with current I at point P, located at a distance d from the wire can be simply estimated according to the Biot-savart law as $B = \mu_0 I / 2\pi d$. Assuming perfect symmetrical windings, the magnetic field distribution around the CT is identical for any primary winding N_p and its associated current I_p as the product $N_p \cdot I_p$ corresponds to the same ampere-turns for a given excitation of the core.

B. Measuring Resistor

The conversion of the secondary current to the output voltage for the measuring system was realised with a resistor box, containing several measuring resistors. The resistor box

provides the required power supply for the CT. Fig. 2 schematically shows the design of the resistor box, which consists of five precision resistors with a maximum power of 3 W each [13], two power supplies and two channels. The integration of the second channel allows to develop easily calibration facilities for another zero-flux current transformer (device under test, CT(X)). The nominal values of the resistors (R_1 to R_5) shown in Fig. 2 were selected from 1 Ω to 20 Ω , according to the nominal load in Table I. Two identically power supplies (PS_1 and PS_2) were located in the resistor box. The power supply operates the CT to the CT's standard work condition with ± 15 V DC voltage. The wiring from the resistor box to the CT was made up with a 4 m long customized cable, containing a coaxial cable for the secondary current and another shielded cable with twisted wires for the power supply.

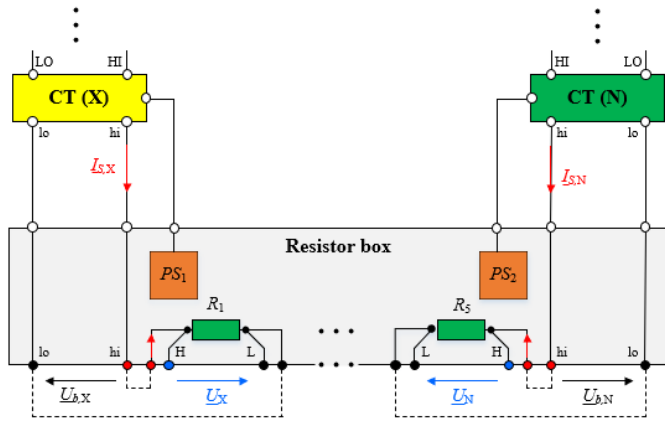


Fig. 2: Connection scheme of the resistor box with the measuring resistors R_1 to R_5 , two power supplies and two CTs. Here, CT (X) and CT (N) refer to the DUT and the reference CT in a potential calibration setup. PS_1 and PS_2 refer to ± 15 V power supplies for X and N.

According to the manufacturer's data sheet, each resistor has been mounted on a heat sink with a thermal resistance of below 4 K/W. Table II shows the calibrated errors (ϵ_m and δ_m) and the corresponding electrical time constants $\tau = \delta_m / \omega$ of the resistors with an output of 1 V at 50 Hz. To realise such small errors of below 0.002 %, the resistors are being adjusted by means of an additional resistor in parallel.

Table II: The measured errors and time constant of the resistors R_1 to R_5 at rated current I_{nom} and at 50 Hz

R_m	I_{nom}	ϵ_m in ppm	δ_m in μ rad	τ in ns
1 Ω	1 A	-11.8	2.6	8
2.5 Ω	400 mA	-12.0	2.2	7
5 Ω	200 mA	-0.7	0.7	2
10 Ω	100 mA	-10.4	0.2	1
20 Ω	50 mA	-11.1	-0.3	-1

The initial measurements with these resistors showed that the errors of the resistors performed not as stable as they were expected from the manufacturer's specification for the temperature coefficient and power coefficient. The observed variation of the error with the test current from 0 to I_{nom} was in range of up to 15 ppm for the 2.5 Ω -resistor. Compared to the manufacturer's specification it should have four times lower variations. This problem of the resistors was discussed with the manufacturer. The result was that all resistors would be

replaced with two resistors per value to lower the power loss inside the resistor and with better matched ones. This replacement is currently in process. Under these circumstances, the measurements in section III, were carried out with other precision resistors.

C. Step-up calibration process of the C-to-V transformers

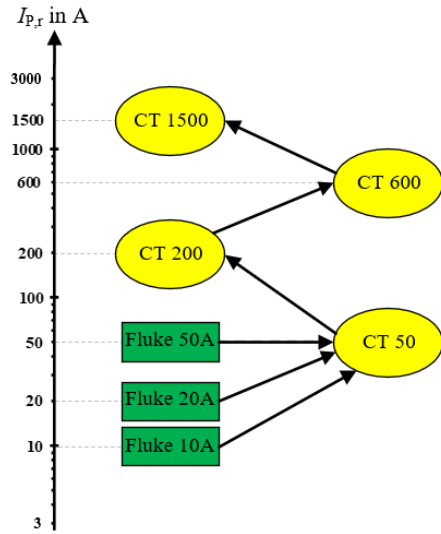


Fig. 3. Step-up calibration of the C-to-V transformer set.

The additional advantage of having several primary symmetrical windings is that, with a high degree of symmetry of the different primary windings, the magnetic field distribution around the used zero-flux CT is identical due to the same ampere-turns. This leads to the situation that the error of the CT is independent of current range in use and makes the calibration convenient, as one symmetrical CT might only be calibrated at the lowest current range. However, this desirable behaviour has to be proved. The scheme shown in Fig. 3 characterizes the step-up calibration principle for the C-to-V transformer set with reference related to the nominal primary current. This principle was especially used when the frequency response of the CTs is determined. At power frequency the CTs could directly be calibrated versus a high accurate standard current transformer. First of all, CT50 was calibrated by using precision and wideband shunts Fluke A40B. After that, the CTs were calibrated step by step against the previously calibrated CT.

III. CHARACTERISATION OF THE C-TO-V TRANSFORMERS

The characterisation of the C-to-V transformers was carried out in such a way that the behaviour at power frequency (section A) and the determination of the frequency response (section B) were done separately. The analysis of the measurement uncertainty is described in section C. This method allows to split the ratio error ϵ_i of the CT into two parts: the basic ratio error $\epsilon_i(f_0)$ at a specific frequency $f_0 = 50$ Hz, and an error difference $\Delta\epsilon_i(f)$ which describes the frequency response with respect to 50 Hz.

$$\epsilon_i = \epsilon_i(f_0) + \Delta\epsilon_i(f) \quad (2)$$

This method allows the uncertainty of the measured frequency response of the C-to-V transformer to be optimised due to the typical drift effects of the high current reference resistors [15] used.

A. Behaviour of the C-to-V transformers at power frequency

The experiments at power frequency concentrate on three aspects: the winding asymmetry, the different current ranges of each CT and the burdening with the measuring resistor. For the calibration, a standard current comparator (*Tettex*) with small ratio and phase errors of below 3 ppm and μrad was adopted as reference. As measurement system a current transformer bridge with uncertainties in the order of 1 ppm and μrad was used [14]. Here only the CT of the C-to-V converter was calibrated. Thus, the additional uncertainties caused by the imperfect measuring resistor R_m could be avoided.

Firstly, three possible primary windings with two turns of the CT50 were measured. As a result, the difference of ratio and phase errors between any measurement was less than 2 ppm and μrad with primary currents from 5 % to 140 %. This difference, which is well within the measurement uncertainty of the used standard CT, might be due to the magnetic field asymmetry of all primary windings. Similarly, CT200 was tested with the four different single turns and a primary current of 5 % to 30 %. Therefore, the min-max difference of ratio and phase errors was less than 4 ppm and 10 μrad .

Secondly, measurements regarding the current ranges focus on the behaviour of the symmetrical CTs with a different number of turns of the primary winding, i.e., $N_p = 1, \dots, 6$ of CT50 and $N_p = 1, \dots, 4$ of CT200. The basic ratio errors $\varepsilon_i(f_0)$ and phase displacement δ_i were measured with primary currents from 5 % to 140 % of the nominal current for CT50 and from 5 % to 120 % of the nominal current for CT200. The variation of the basic ratio errors in each measurement is within $\pm 1 \mu\text{A}/\text{A}$ and $\pm 0.5 \mu\text{rad}$ with different primary currents from 5 % to 120 % or 140 % of the rated current range in use.

Table III: Basic ratio and phase errors of CT50 and CT200 at 50 Hz. The results are given for a nominal current of CT50 with a 0.5 Ω burden and of CT200 with a 0.1 Ω burden.

No. of turns N_p	CT50		CT200	
	ε_i in $\mu\text{A}/\text{A}$	δ_i in μrad	ε_i in $\mu\text{A}/\text{A}$	δ_i in μrad
1	-2.2	-1.6	-9.2	-4.2
2	-1.8	0.3	-8.1	-4.9
3	-1.5	0.5	-8.1	-4.2
4	-1.9	-0.1	-9.5	-4.7
5	-2.2	-0.3		
6	-2.5	-0.3		
average	-2.0	-0.3	-8.7	-4.5

The measuring errors ε_i and δ_i are given in Table III for each current range via the number of turns (N_p) and at the nominal current (100 %) of CT50 and CT200 only. It is apparent that the basic ratio error and the phase displacement are practically unaffected by the used number of turns.

Finally, measurements were performed with three different burdens of the CT. The resistance values listed in Table IV represent the burden resistors and the obtained basic ratio and phase error of the CT.

Table IV: Basic ratio and phase errors of CT50 and CT200 at 50 Hz with various burdens R_B . The results are given at a nominal current for CT50 with 5 turns and for CT200 with 4 turns.

CT50; $N_p = 5$; $I_p = 10 \text{ A}$			CT200; $N_p = 4$; $I_p = 50 \text{ A}$		
R_B in Ω	ε_B in $\mu\text{A}/\text{A}$	δ_B in μrad	R_B in Ω	ε_B in $\mu\text{A}/\text{A}$	δ_B in μrad
0.5	-2.2	-0.3	0.1	-9.5	-4.7
5.5	-3.1	-1.9	2.6	-9.9	-5.2
10.5	-4.1	-3.7	5.1	-10.7	-6.1

The results presented in Table IV prove that the measured errors of CT have a linear relationship with the burden at 50 Hz. With an increase in a burden resistance of 5 Ω , the errors of CT50 decreased by approximately 1 ppm and 1.4 μrad . With an increase in a burden resistance of 2.5 Ω , the errors of CT200 decreased by approximately 0.5 ppm and 0.7 μrad .

B. Frequency Response of the C-to-V transformers

Fig. 4 shows the detailed measurement arrangement for calibrating the wideband frequency response of the C-to-V transformer set. This consists of two CTs, the reference CT (N) and DUT (X), with corresponding load (R_N and R_X) and an AC voltage ratio measuring system (VRS) [14], [15]. The input current I_p flows through the primary side of N and X. The load resistors R_N and R_X convert the secondary currents of N and X into the respective output voltages measured by the VRS.

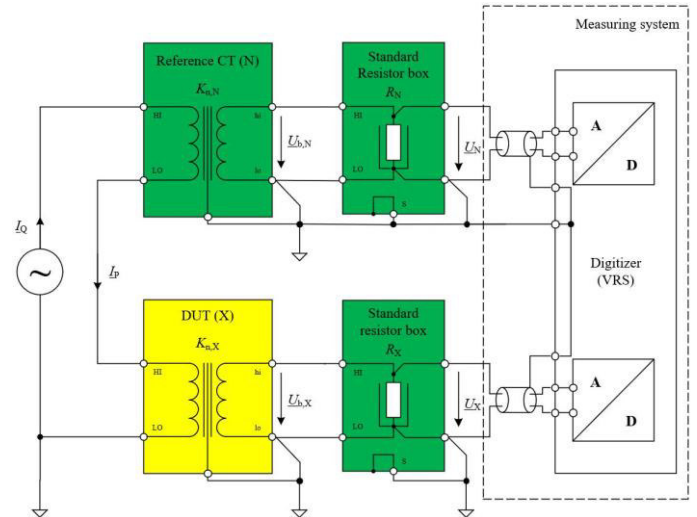


Fig. 4: Calibration scheme of the C-to-V transformer set. In practice, the reference CT (N) refers to the highly stable measuring resistor set Fluke A40B with a nominal current of 10A / 20A / 50A / 100A or the calibrated CT50 / 200 / 600; the device under test (DUT(X)) refers to CT50 / 200 / 600 / 2000 to be calibrated, the secondary resistors R_N and R_X are selected from the resistor box shown in Fig. 2.

From the complex voltage ratio $\underline{I}_{XN} = U_X / U_N$, the ratio error ε_i and phase error δ_i of the CT under test (DUT X) were evaluated. The evaluation of the frequency response consists of three aspects: the linearity of the CT at different primary currents, the error differences with different current ranges in use and the burdening of the CT. The measured frequency response $\Delta\varepsilon_i(f)$ and $\delta_i(f)$ for the CT50 and CT200, which is the difference of the measured ratio and phase errors $\varepsilon_i(f) - \varepsilon_i(50 \text{ Hz}) - \text{see (2)} -$ are displayed by curves in Fig. 5 and

Fig. 6. The frequency range in the calibration is from 16 Hz to 12 kHz. The involved time constant of the calibrated reference resistor set is known and in the order of some nanoseconds. Knowledge of the time constant is especially important for calculating the phase error of the CTs under test.

Firstly, measurements between 20 % and 80 % of the nominal current at rated burden showed that the error difference ($|\Delta\varepsilon_{i,20\%}(f) - \Delta\varepsilon_{i,80\%}(f)|$ and $|\Delta\delta_{i,20\%}(f) - \Delta\delta_{i,80\%}(f)|$) of CT50 was below 50 ppm and 5 μrad and below 15 ppm and 10 μrad for the CT200 at 12 kHz. Compared to the errors at 12 kHz, these differences can be considered small and will be used as uncertainty contribution.

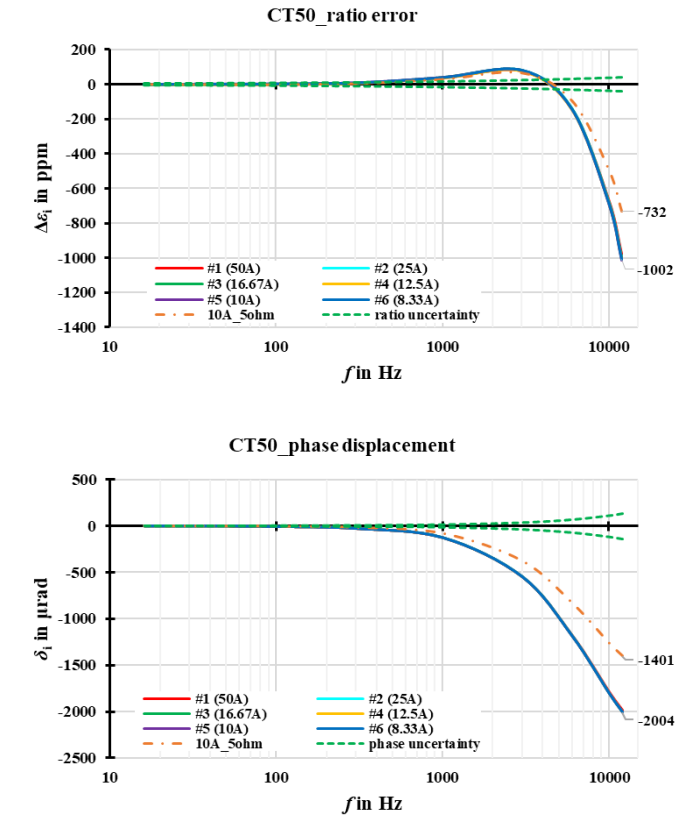


Fig. 5: Frequency response of the ratio errors in the different current ranges of the CT 50 against the measuring resistor set Fluke A40B. Measured results are given for 80 % of the nominal current of CT50. The six solid curves represent the results $\Delta\varepsilon_i(f)$ and $\delta_i(f)$ for $N_p = 1$ (50 A) to $N_p = 6$ (8.33 A) with a 10 Ω measuring resistor. The semicolon curve (orange) represents the errors at $N_p = 5$ ($I_p = 10\text{A}$) with a 5 Ω measuring resistor. The two mirrored dashed curves (green) represent the calculated standard uncertainties.

Secondly, measurements of the frequency responses were carried out in the different current ranges of CT50 and of CT200. For CT50, it was calibrated, according to the calibration setup in Fig. 4, directly by highly stable current shunts [9] with the nominal current of 10 A, 20 A and 50 A. The results of the frequency response errors with their calculated measurement uncertainties are shown in Fig. 5 for the different current ranges from 8.33 A to 50 A and with a 10 Ω measuring resistor. Almost identical frequency responses can be obtained for all current ranges. Up to 12 kHz the ratio errors and the phase errors are below 0.1 % and 0.2 crad. By lowering the burden to

5 Ω , the errors decrease to below 0.07 % and 0.1 crad at 12 kHz. However, the errors from 16 Hz to 300 Hz are enormously stable and approximately zero. The measurement uncertainties (see section C) increase with higher frequencies. At 12 kHz they reach the highest standard uncertainties $u(\Delta\varepsilon_i(f)) = \pm 4 \cdot 10^{-5}$ for the frequency response of the ratio error and $u(\delta_i(f)) = \pm 1.3 \cdot 10^{-4}$ for the phase error $\delta_i(f)$, respectively.

The CT200 (DUT X) was calibrated with the CT50, which now behaves as the reference N according to the measurement setup in Fig. 4. The frequency response errors of CT200 are shown in Fig. 6.

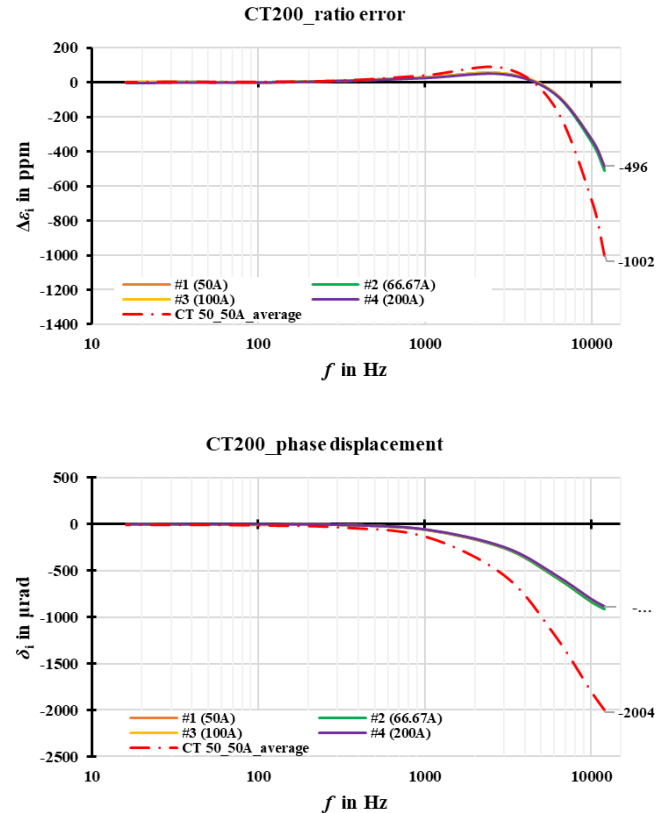


Fig. 6: Frequency response of the ratio errors in the different current ranges of the CT 200 against CT 50. Measured results are given for 80 % of the nominal current of CT50. The four solid curves represent the results $\Delta\varepsilon_i(f)$ and $\delta_i(f)$ for $N_p = 1$ (200 A) to $N_p = 4$ (50 A) with a 2.5 Ω measuring resistor. The semicolon curve (red) represents the averaged frequency response of the CT50.

The results show that for all current ranges from 50 A ($N_p = 4$) to 200 A ($N_p = 1$) of the CT200, with a 2.5 Ω measuring resistor, almost identical frequency responses can be obtained. Up to 12 kHz the ratio errors and the phase errors are below 0.05 % and 0.1 crad. For comparison purposes, the averaged frequency responses of CT50 are given too, which clearly shows that the CT200 exhibits approximately half the errors of CT 50. The errors from 16 Hz to 300 Hz are enormously stable and approximately zero.

Thirdly, in order to figure out the plausibility of the calibration of the symmetrical CTs according to the proposed step-up procedure (see Fig. 3), further observations were done with the CT200. The calibration with the high current shunt has

been repeated at 50 Hz and 12 kHz. From these measurements, the frequency response $\Delta\varepsilon_i(12 \text{ kHz})$ and the phase $\delta_i(12 \text{ kHz})$ has been calculated. Comparing these results at 12 kHz with the results obtained with the CT50 (see Fig. 6), indicate differences (residuals) of not more than $20 \mu\text{A} / \text{A}$ and $10 \mu\text{rad}$.

C. Measurement Uncertainty of the C-to-V transformers

The CT50 is considered as the reference for the wideband C-to-V transformer set. According to the error definition shown in (2), the standard uncertainties consist of a basic uncertainty $u(\varepsilon_i(f_0))$ at 50 Hz, and the frequency response uncertainties $u(\Delta\varepsilon_i(f))$ for the ratio errors and $u(\delta_i(f))$ for the phase errors. The standard uncertainty at 50 Hz is determined to be $\pm 1.7 \cdot 10^{-6}$ for the ratio and for the phase error. The combined standard measurement uncertainties for the frequency responses, e.g. $u(\Delta\varepsilon_i(f))$, of the CT50 for any frequency f (within 12 kHz) are calculated by

$$u(\Delta\varepsilon_i(f)) = \sqrt{u_w(\varepsilon_i(f))^2 + u_M(\varepsilon_i(f))^2 + u_F(f)^2 + u_{MF}(f)^2} \quad (3)$$

with the corresponding individual standard uncertainties of:

- results averaging between different winding setups $u_w(\varepsilon_i(f))$,
- model simulation uncertainty $u_M(\varepsilon_i(f))$,
- current shunt Fluke A40B as the reference N $u_F(f)$
- magnetic field influence between N and X (measuring position of N and X) $u_{MF}(f)$.

The measurement uncertainties of $u(\delta_i(f))$ follow the same calculation shown in (3). As a result, the calculated measurement uncertainties $u(\varepsilon_i(f))$ and $u(\delta_i(f))$, taking account of the standard uncertainty at 50 Hz, can be tabulated for the different frequencies. The uncertainties increase with the increasing frequency. Two characteristic measurement uncertainties of the CT50 are listed in Table V.

Table V: Calculated standard uncertainties of the CT50 at 50 Hz and 12 kHz

f in Hz	$u_\varepsilon(\varepsilon_i(f))$ in ppm	$u_\delta(\delta_i(f))$ in μrad
12000	± 40	± 135
50	± 3.5	± 2.8

The measurement uncertainties of CT200, CT600, and CT1500 will be calculated in a similar manner based on their calibration reference CT (see Fig. 3) according to (4). For the operation of the C-to-V transformer, the calibrated measuring resistor R_m and the uncertainties of R_m , $u(\varepsilon_m)$ and $u(\delta_m)$ – see (1) –, are still needed. Finally, the complete uncertainties of the C-to-V transformer will be estimated, combining the uncertainties of $u(\varepsilon_i(f))$ and $u(\delta_i(f))$ and the uncertainties of $u(\varepsilon_m)$ and $u(\delta_m)$.

IV. CONCLUSION

A set of symmetrical C-to-V transformers have been realized as a reference system for calibrating any current transformer, either analogue or digital, as planned in the FutureGrid II project. The rated current ranges are from around 10 A to 1500 A. The errors within the frequency up to 12 kHz

are below 0.1 % and 0.2 crad. The attained expanded uncertainties are below 100 ppm and 300 μrad ($k = 2$).

Further developments of CT600 and CT1500 are currently in process and calibrations of the integrated C-to-V transformer set will be accomplished in the prospective work. Moreover, to reduce the CT errors of the C-to-V transformer, an electronic burden compensation is intended to be integrated in the future.

ACKNOWLEDGMENT

This project has received funding from the EMPIR programme co-financed by the Participating States and from the European Union's Horizon 2020 research and innovation programme.

REFERENCES

- [1] (2017) The Future Grid II website [Online]. Available: <https://www.vtt.fi/sites/FutureGrid2/> [July 2019].
- [2] G. Rietveld, J-P. Braun, P.S. Wright and N. Zisky: "Measurement infrastructure for observing and controlling smart electrical grids," in *29th Conference on Precision Electromagnetic Measurements*, Oct. 2014.
- [3] A. J. Collin, A. Delle Femine, D. Gallo, R. Langella, M. Luiso, "Compensation of Current Transformers' Non-Linearities by Means of Frequency Coupling Matrices," *IEEE Transactions on Instrumentation and Measurement*, pp. 1-9, May 2019.
- [4] A. Cataliotti, V. Cosentino, G. Crotti, A. D. Femine, D. Di Cara, D. Gallo, D. Giordano, C. Landi, M. Luiso, M. Modarres and G. Tinè, "Compensation of Nonlinearity of Voltage and Current Instrument Transformers," *IEEE Transactions on Instrumentation and Measurement*, pp. 1322 - 1332, Dec. 2018.
- [5] *Instrument Transformers - Part 9: Digital interface for instrument transformers*, IEC 61869-9, 2016.
- [6] *Instrument Transformers - Part 13: Stand-alone merging unit (SAMU)*, IEC 61869-13, 2019.
- [7] *Instrument transformers - Part 105: Uncertainty evaluation in the calibration of Instrument Transformers*, IEC 61869-105, 2018.
- [8] Jaeger, Marc. (2018, August 30). Untersuchung zeitsynchronisierter Abtastverfahren zur Bewertung digitaler Wandler nach IEC 61850-9-2, Zenodo, <https://zenodo.org/record/2628462>
- [9] Stromshunts der Serie A40B webpage on FLUKEAL [Online]. Available: <https://eu.flukecal.com/de/products/electrical-calibration/electrical-standards/stromshunts-der-serie-a40b-0> [July 2019].
- [10] M. Cerqueira Bastos: "High Precision Current Measurement for Power Converters," *Proceedings of the 2014 CAS - CERN Accelerator School: Power Converters, Baden, Switzerland*, pp.353-362, May 2014.
- [11] 0A to 600A webpage on DANISENSE [Online]. Available: <https://www.danisense.com/products/0a-to-600a> [July 2019].
- [12] 600A to 3000A webpage on DANISENSE [Online]. Available: <https://www.danisense.com/products/600a-to-3000a> [July 2019].
- [13] VHP4Z & VPR247Z webpage on VISHAYPG [Online]. Available: <http://www.vishaypg.com/foil-resistors/list/product-63239/> [July 2019].
- [14] E. Mohns, J. Meisner, G. Roeissle, and M. Seckelmann, "A Wideband Current Transformer Bridge," *IEEE Trans. Instrum. Meas.*, vol. 63, No. 10, pp. 2322-2329, Oct. 2014.
- [15] E. Mohns, C. Yue, F. Zhou, T. Möhring, and M. Schmidt, "A Current Transformer Test Set for the Audio Frequency Range," in *CPEM 2012 Digest*, Washington, July 2012.